In situ assembly of gold nanoparticles on nitrogen-doped carbon nanotubes for sensitive immunosensing of microcystin-LR†

Jing Zhang, Jianping Lei, Rong Pan, Chuan Leng, Zheng Hu and Huangxian Ju*

Received 2nd October 2010, Accepted 1st November 2010
DOI: 10.1039/c0cc04198j

A simple and green method was developed for *in situ* assembly of gold nanoparticles on nitrogen-doped carbon nanotubes, and the resulting Au/nitrogen-doped carbon nanotubes nanocomposite was used as an immobilization scaffold of antibody for sensitive immunosensing of microcystin-LR.

Nitrogen-doped carbon nanotubes (CNx-MWNTs), as a defective bamboo-like structure with distinctive compartment layers, have attracted considerable attention due to their unique properties and wide applications.[1] Compared with carbon nanotubes (CNTs), CNx-MWNTs have a larger surface-active groups-to-volume ratio, superb thermal stability, and good electrical and mechanical properties.[2a,b] The lower cytotoxicity and better biocompatibility of CNx-MWNTs than un-doped CNTs make them suitable to construct biosensors.[2c,d] Moreover, the incorporation of nitrogen atoms efficiently introduces chemically active sites into the CNx-MWNTs nanotubes for catalytic reactions[3] and the anchoring of metal nanoparticles.[4] Typically, Pt[4a] and Ni[4b] nanoparticles have been successfully immobilized on CNx-MWNTs by the ethylene glycol method.

By functionalization of CNx-MWNTs with polyelectrolyte, gold nanoparticles (AuNPs) have also been selectively anchored on their surface *via* electrostatic interactions.[5] To simplify the functionalization process, this work developed a convenient and green chemical route to directly attach AuNPs onto CNx-MWNTs, and the resulting Au/CNx-MWNTs nanocomposite was used as an immobilization scaffold of antibodies for preparation of a sensitive immunosensor for microcystin-LR (Scheme 1).

Microcystin-LR (MC-LR), containing five nonproteinogens and two substitutions of leucine (L) and arginine (R) at positions 2 and 4, is the most toxic species of the cyanotoxins.[6] In 1998, the World Health Organization (WHO) set up a provisional guideline limit of 1 μg L^{-1} for MC-LR in drinking water.[7] Thus, the recognition and quantification of MC-LR are of great importance in the analysis of environmental samples. Several methods such as thin-layer chromatography,[8] high-performance liquid chromatography,[9] liquid chromatography-mass spectrometry[10] and protein phosphatase inhibition assays[11] have been developed for determination of MC-LR. Although these methods are widely accepted, they require relatively expensive equipment, advanced technical expertise, high cost and are time consuming. Particularly, it is difficult to use these methods for *in situ* or online monitoring. This work provided a low-cost method for convenient detection of MC-LR. Compared with those based on immunosensors, this method showed a wider concentration range and lower limit.

Fig. 1 shows the typical transmission electron micrograph (TEM) images of Au/CNx-MWNTs and Au/multi-walled carbon nanotubes (Au/MWNTs) prepared by the same method in parallel experiments. AuNPs with sizes of 3–7 nm were homogeneously dispersed on the surface of the CNx-MWNTs, forming a hybrid structure of Au/CNx-MWNTs (Fig. 1A). In contrast, AuNPs could not be efficiently dispersed on MWNTs (Fig. 1B). The aggregation phenomenon of AuNPs resulted from the chemical inertness of the regular MWNTs. The result suggested a strong interaction between AuNPs and CNx-MWNTs, which is caused by the N-participation in their connection, similar to the cases of immobilizing Ag, Ni and Pt nanoparticles on CNx-MWNTs.[4]

The X-ray diffraction (XRD) studies of CNx-MWNTs showed two peaks at 26.0° and 46.7° assigned to (002) and (100) planes of graphite, respectively (curve a, Fig. S1 in ESI†). The additional peaks of Au/CNx-MWNTs at 38.4°, 44.5°, 64.8° and 77.3° were assigned to the (111), (200), (220) and (311) planes of AuNPs, respectively (curve b, Fig. S1 in ESI†), indicating a face-centered cubic structure.[12] After *in situ* assembly of AuNPs, the weak graphite (100) peak became invisible due to the overlapping with the strong Au (111) and (200) peaks. Therefore, the XRD results suggested that the reduction process by $NaBH_4$ produced metallic state Au species with good crystallinity on CNx-MWNTs.

X-Ray photoelectron spectra (XPS) were recorded to further analyze the chemical composition and status of the CNx-MWNTs and Au/CNx-MWNTs (Fig. S2A in ESI†).

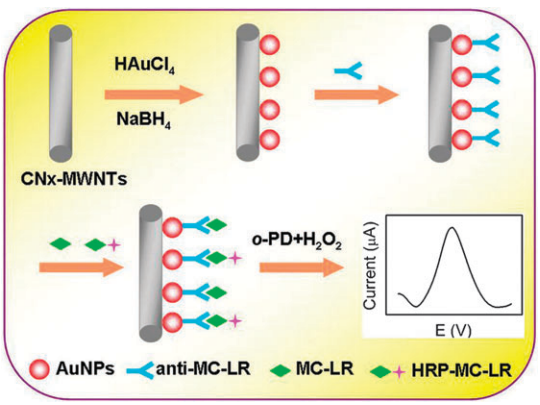

Scheme 1 Schematic representation of the preparation and detection procedure of MC-LR immunosensor.

Key Laboratory of Analytical Chemistry for Life Science (Ministry of Education of China), Department of Chemistry, Nanjing University, Nanjing 210093, P.R. China. E-mail: hxju@nju.edu.cn; Fax: +862583593593; Tel: +862583593593

† Electronic supplementary information (ESI) available: Experimental details, characterization of Au/CNx-MWNTs, and optimal conditions for immunoreaction and detection. See DOI: 10.1039/c0cc04198j

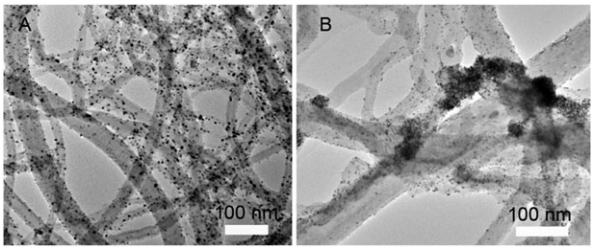

Fig. 1 TEM images of (A) Au/CNx-MWNTs and (B) Au/MWNTs.

The XPS survey spectrum of CNx-MWNTs displayed C 1s and N 1s with an N content of about 3.7%. In contrast, the XPS survey spectrum of Au/CNx-MWNTs exhibited distinct Au 4f peaks at binding energy of 84.2 eV and 87.9 eV (Fig. S2B in ESI†), which corresponded to Au $4f_{7/2}$ and $4f_{5/2}$, respectively.[13] This result further confirmed the formation of metallic Au on the Au/CNx-MWNTs surface.

AuNPs as an immobilized matrix can firmly bind antibodies through ionic interactions and other interactions between AuNPs and mercapto or primary amine groups of antibodies.[14] Considering the advantages of AuNPs and CNx-MWNTs, and the homogeneous dispersion of AuNPs on CNx-MWNTs, an immunosensor of MC-LR was designed by immobilizing the MC-LR antibody (anti-MC-LR) on the Au/CNx-MWNTs composite modified glassy carbon electrode (GCE). The immunoassay could be carried out by a competitive immunoreaction of the immobilized MC-LR antibody with MC-LR and horseradish peroxidase labeled MC-LR (HRP-MC-LR) (Scheme 1). In 0.2 M phosphate buffer saline (PBS), HRP-MC-LR/anti-MC-LR/(Au/CNx-MWNTs)/GCE did not show any detectable signal in the working potential range (curve a, Fig. 2), though it showed a slightly larger background current than HRP-MC-LR/anti-MC-LR/(Au/MWNTs)/GCE (curve b, Fig. 2) and HRP-MC-LR/anti-MC-LR/CNx-MWNTs/GCE (curve c, Fig. 2). When *o*-phenylenediamine (*o*-PD) and H_2O_2 were added into PBS, the cyclic voltammogram of HRP-MC-LR/anti-MC-LR/(Au/CNx-MWNTs)/GCE exhibited a pair of stable and well-defined redox peaks at −0.554 and −0.618 V (curve d, Fig. 2), which corresponded to the redox of 2,2′-diaminoazobenzene, the enzymatic product.[15] Although these peaks also

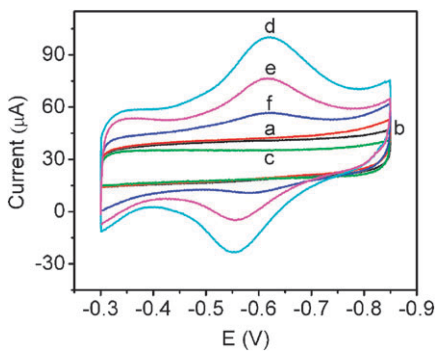

Fig. 2 Cyclic voltammograms of HRP-MC-LR/anti-MC-LR/(Au/CNx-MWNTs)/GCE (a, d), HRP-MC-LR/anti-MC-LR/(Au/MWNTs)/GCE (b, e) and HRP-MC-LR/anti-MC-LR/CNx-MWNTs/GCE (c, f) in 0.2 M pH 7.0 PBS in the absence (a, b, c) and presence (d, e, f) of 8.0 mM H_2O_2 and 10 mM *o*-PD. Scan rate: 60 mV s^{-1}.

occurred for HRP-MC-LR/anti-MC-LR/(Au/MWNTs)/GCE (curve e, Fig. 2) and HRP-MC-LR/anti-MC-LR/CNx-MWNTs/GCE (curve f, Fig. 2), the peak currents were 2 and 7 times lower than those of HRP-MC-LR/anti-MC-LR/(Au/CNx-MWNTs)/GCE, respectively, indicating the significant sensitizing effect of Au/CNx-MWNTs. The sensitizing effect could benefit from the homogeneous dispersion of AuNPs on CNx-MWNTs for binding of anti-MC-LR and easy recognition of bound anti-MC-LR to HPR-MC-LR, which would lead to enhanced sensitivity for the proposed MC-LR immunosensor.

The electrochemical response depends on the formation of an immunocomplex on the electrode surface. The latter is decided by the concentration of HRP-MC-LR in the incubation solution and incubation time. In order to obtain the optimal concentration of HRP-MC-LR, the anti-MC-LR/(Au/CNx-MWNTs)/GCEs were incubated in HRP-MC-LR solutions with different concentrations. The peak current increased with increasing HRP-MC-LR concentration and tended to a plateau at 10 μg mL^{-1}, indicating that all the available recognition sites of immobilized anti-MC-LR were matched with the enzyme conjugate (Fig. S3A in ESI†). Thus, 10 μg mL^{-1} of HRP-MC-LR was used for the incubation step.

At the optimized HRP-MC-LR concentration, with the incubation time increasing from 5 to 60 min the immunosensor showed an increasing response until an incubation time of 20 min (Fig. S3B in ESI†). Longer incubation time did not obviously improve the response. Therefore, an incubation time of 20 min was chosen as the optimal incubation condition for the immunoassay of MC-LR.

For the measurement of MC-LR, a competitive assay configuration was applied under optimized conditions. A standard solution of MC-LR at a known concentration was added into the incubation solution containing a certain concentration of HRP-MC-LR. The MC-LR and HRP-MC-LR in the incubation solution competed with the limited binding sites of the immobilized anti-MC-LR on the immunosensor surface to form an immunocomplex. The captured HRP-MC-LR on the immunosensor surface then catalyzed the oxidation of *o*-PD by H_2O_2 to produce 2,2′-diaminoazobenzene. The optimal concentrations of *o*-PD and H_2O_2 were selected to be 10 mM (Fig. S4A in ESI†) and 8 mM (Fig. S4B in ESI†), respectively. The differential pulse voltammetric (DPV) peak current of 2,2′-diaminoazobenzene decreased with the increasing MC-LR concentration in the incubation solution (Fig. 3A). As shown in Fig. 3B, the decrease of the DPV peak current was proportional to the MC-LR concentration in the range of 0.005–1.00 μg L^{-1} with a correlation coefficient of 0.9997. This result was much wider than those of 0.03–3.16 μg L^{-1} for a competitive binding electrochemical enzyme immunoassay,[16a] 0.06–0.65 μg L^{-1} for a chemiluminescence enzyme immunoassay,[16b] and 0.1–10.1 μg L^{-1} for a portable optical immunosensor.[16c] The detection limit was calculated to be 0.002 μg L^{-1} at a signal-to-noise ratio of 3, which was much lower than 0.03 μg L^{-1} for a carbon nanohorns-based immunosensor[16d] and the WHO provisional guideline limit of 1 μg L^{-1} for MC-LR in drinking water.[7] According to the analytical process, the detectable linear range in the sample with a dilution factor of 2 by adding 10 μL HRP-MC-LR was 0.01-2 μg L^{-1} with a

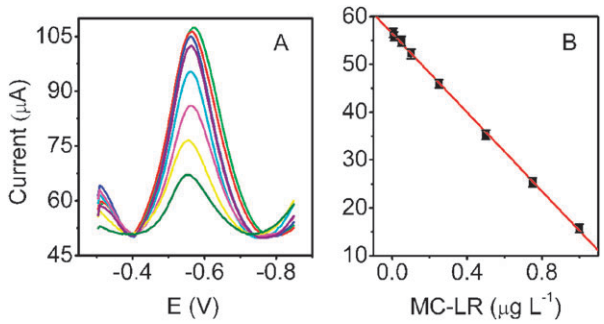

Fig. 3 (A) DPV response of the immunosensor in 0.2 M pH 7.0 PBS containing 10 mM *o*-PD and 8 mM H_2O_2 after incubation with 0.005, 0.01, 0.05, 0.10, 0.25, 0.5, 0.75 and 1 μg L^{-1} MC-LR (from highest to lowest peak currents) and (B) calibration curve for MC-LR immunoassay.

detection limit of 0.004 μg L^{-1}. Thus the proposed method was enough for practical application.

The coefficients of variation for five repeated measurements with this method were 2.8% and 4.8% at MC-LR concentrations of 0.025 and 0.75 μg L^{-1}, respectively, showing good reproducibility. The MC-LR immunosensor also showed good fabrication reproducibility with relative standard deviations of 3.2% and 5.1% at MC-LR concentrations of 0.025 and 0.75 μg L^{-1} on five independently made immunosensors. When the immunosensor was not in use, it was stored at 4 °C. 96.1% of the initial response of the immunosensor for MC-LR remained after one week and 82.3% of the initial response remained after four weeks. These results indicated the immunosensor had acceptable stability. The immunosensor could be renewed by rinsing with stripping buffer of pH 2.8 glycine–HCl solution to dissociate the antigen–antibody complex. The as-renewed immunosensor could restore 92.4% of the initial value after five assay runs, showing good reusability.

To evaluate the analytical reliability and application potential of the proposed method, 10 μL of water samples, without any need of sample pretreatment except appropriate dilution with PBS, was mixed with 10 μL HRP-MC-LR, and the mixture was dropped on the MC-LR immunosensor. The MC-LR concentrations determined with this method were 1.25 ± 0.05 and 5.3 ± 0.2 μg L^{-1}. Recovery testing was carried out to demonstrate the validity of the proposed method, after 0.2 μg L^{-1} of MC-LR was added to two samples, and the obtained recoveries of MC-LR were $95.1 \pm 1.2\%$ and $96.2 \pm 2.0\%$, respectively (after five measurements), which indicated acceptable accuracy. Thus, the present method could satisfy the need for immunoassay of MC-LR in water samples.

In summary, this work presented a convenient and green method to directly attach AuNPs on CNx-MWNTs without the need for surface modification due to the inherent chemical activity of CNx-MWNTs. AuNPs were well dispersed and strongly anchored on the surface of CNx-MWNTs through the N-participation in their connection. By immobilizing anti-MC-LR on the surface of the Au/CNx-MWNTs composite modified GCE, an immunosensor was constructed for detection of MC-LR. The immunosensor showed wide linear range, low detection limit, good reproducibility and acceptable long-term stability, and could successfully detect MC-LR in polluted water samples. The Au/CNx-MWNTs nanocomposite provided a biocompatible platform for biosensing and biocatalysis.

This work was funded by National Basic Research Program of China (2010CB732400), National Natural Science Foundation of China (20821063, 90713015, 20875044, 20835006), and Natural Science Foundation of Jiangsu (BK2008014).

Notes and references

1 (*a*) W. C. Fang and W. L. Fang, *Chem. Commun.*, 2008, 5236–5238; (*b*) G. Vijayaraghavan and K. J. Stevenson, *Langmuir*, 2007, **23**, 5279–5282.
2 (*a*) V. H. Ebron, Z. W. Yang and D. J. Seyer, *Science*, 2006, **311**, 1580–1583; (*b*) K. P. Gong, F. Du, Z. H. Xia, M. Durstock and L. M. Da, *Science*, 2009, **323**, 760–764; (*c*) J. C. Carrero-Sánchez, A. L. Elías, R. Mancilla, G. Arrellín, H. Terrones, J. P. Laclette and M. Terrones, *Nano Lett.*, 2006, **6**, 1609–1616; (*d*) A. L. Elías, J. C. Carrero-Sánchez, H. Terrones, M. Endo, J. P. Laclette and M. Terrones, *Small*, 2007, **3**, 1723–1729.
3 S. van Dommele, K. P. de Jong and J. H. Bitter, *Chem. Commun.*, 2006, (46), 4859–4861.
4 (*a*) B. Yue, Y. W. Ma, H. S. Tao, L. S. Yu, G. Q. Jian, X. Z. Wang, X. S. Wang, Y. N. Lu and Z. Hu, *J. Mater. Chem.*, 2008, **18**, 1747–1750; (*b*) S. H. Yang, W. H. Shin, J. W. Lee, H. S. Kim and J. K. Kang, *Appl. Phys. Lett.*, 2007, **90**, 013103.
5 K. Y. Jiang, A. Eitan, L. S. Schadler, P. M. Ajayan, R. W. Siegel, N. Grobert, M. Mayne, M. Reyes-Reyes, H. Terrones and M. Terrones, *Nano Lett.*, 2003, **3**, 275–277.
6 (*a*) M. Welker, M. Brunke, K. Preussel, I. Lippert and H. Von Döhren, *Microbiology*, 2004, **150**, 1785–1796; (*b*) K. L. Howard and G. L. Boyer, *Anal. Chem.*, 2007, **79**, 5980–5986.
7 WHO. Guidelines for Drinking-Water Quality. Addendum to Volume 2. Health Criteria and Other Supporting Information; World Health Organization: Geneva, Switzerland, 1998.
8 I. Meisen, U. Distler, J. Müthing, S. Berkenkamp, K. Dreisewerd, W. Mathys, H. Karch and M. Mormann, *Anal. Chem.*, 2009, **81**, 3858–3866.
9 L. Spoof, K. Karlsson and J. Meriluoto, *J. Chromatogr., A*, 2001, **909**, 225–236.
10 M. Maizels and W. L. Budde, *Anal. Chem.*, 2004, **76**, 1342–1351.
11 M. Campàs, D. Szydlowska, M. Trojanowicz and J. L. Marty, *Biosens. Bioelectron.*, 2005, **20**, 1520–1530.
12 C. Xu, X. Wang and J. W. Zhu, *J. Phys. Chem. C*, 2008, **112**, 19841–19845.
13 Y. Shi, R. Z. Yang and P. K. Yuet, *Carbon*, 2009, **47**, 1146–1151.
14 (*a*) R. J. Cui, H. C. Pan, J. J. Zhu and H. Y. Chen, *Anal. Chem.*, 2007, **79**, 8494–8501; (*b*) Y. Zhuo, P. X. Yuan, R. Yuan, Y. Q. Chai and C. L. Hong, *Biomaterials*, 2009, **30**, 2284–2290.
15 J. Chen, F. Yan, D. Du, J. Wu and H. X. Ju, *Electroanalysis*, 2006, **18**, 670–676.
16 (*a*) F. Zhang, S. H. Yang, T. Y. Kang, G. S. Cha, H. Nam and M. E. Meyerhoff, *Biosens. Bioelectron.*, 2007, **22**, 1419–1425; (*b*) F. Long, H. C. Shi, M. He, J. W. Sheng and J. F. Wang, *Anal. Chim. Acta*, 2009, **649**, 123–127; (*c*) F. Long, M. He, A. N. Zhu and H. C. Shi, *Biosens. Bioelectron.*, 2009, **24**, 2346–2351; (*d*) J. Zhang, J. P. Lei, C. L. Xu, L. Ding and H. X. Ju, *Anal. Chem.*, 2010, **82**, 1117–1122.

Electronic Supplementary Information (ESI) for Chemical Communications

In situ assembly of gold nanoparticles on nitrogen-doped carbon nanotubes for sensitive immunosensing of microcystin-LR

Jing Zhang, Jianping Lei, Rong Pan, Chuan Leng, Zheng Hu and Huangxian Ju*

Key Laboratory of Analytical Chemistry for Life Science (Education Ministry of China), Department of Chemistry, Nanjing University, Nanjing 210093, P.R. China

Experimental

Materials and Reagents. Nitrogen-doped carbon nanotubes (CNx-MWNTs) were synthesized according to the previously reported method,[1] and were further refluxed in 6 M NaOH at 110 °C for 4 h to remove the Al_2O_3 support, followed by refluxing in 1 M H_2SO_4 for 8 h to remove residual Fe catalysts.[2] The purified CNx-MWNTs was thoroughly washed with double-distilled water until the pH value of the filtrate reached 7, and then dried at 70 °C overnight for further study. Multi-walled carbon nanotubes (MWNTs) were obtained from Shenzhen Nanotech Port Company. Microcystin-LR (MC-LR), MC-LR antibody (anti-MC-LR) and horseradish peroxidase (HRP) labeled MC-LR (HRP-MC-LR) were purchased from Express Technology Co., Ltd (China). Bovine serum albumin (BSA) was obtained from Sigma (St. Louis, MO). All other reagents, including H_2O_2 and o-phenylenediamine (o-PD), were of analytical grade. Blocking buffer was 0.01 M pH 7.4 phosphate buffer saline (PBS) containing 2% BSA. To minimize unspecific adsorption, 0.05% Tween-20 was spiked into PBS as wash buffer (PBST). The detection buffer was 0.2 M pH 7.4 PBS. Ultrapure water obtained from a Millipore water purification system (≥ 18 MΩ, Milli-Q, Millipore) was used in all runs. The polluted water samples were from Tai lake in Wuxi, China.

Preparation of Au/CNx-MWNTs Nanocomposite. 7 mg CNx-MWNTs was dispersed in 40 mL aqueous solution containing 2.5×10^{-4} M trisodium citrate and then sonicated for 30 min. 0.4 mL 1% $HAuCl_4\cdot3H_2O$ was added to the solution and stirred for 10 min. 1.2 mL of 0.1 M ice cold $NaBH_4$ solution was added to the mixture solution under stirring at 0 °C. After stirring for an additional 2 h, the black solid was separated by centrifuging at a speed of 10000 rpm, washed with water for several cycles, and then dried overnight at 80 °C.

Preparation of MC-LR Immunosensor. The glassy carbon electrode (GCE, 3 mm diameter) was polished successively with 0.3- and 0.05-μm alumina slurry (Beuhler) followed by rinsing thoroughly with doubly distilled water. After successive sonication in 1:1 nitric acid, acetone and deionized water, the electrode was rinsed with deionized water and allowed to dry at room temperature. 6 μL of 2 mg mL^{-1} Au/CNx-MWNTs suspension was dropped on the pretreated GCE and dried in a desiccator. 10 μL of 1 μg mL^{-1} anti-MC-LR was dropped on its surface and then incubated for 12 h to form anti-MC-LR/(Au/CNx-MWNTs)/GCE. Following a rinse with 0.01 M pH 7.4 PBST, the formed immunosensor was blocked with 0.01 M pH 7.4 PBS containing 2% BSA for 30 min. After thorough washing with 0.01 M pH 7.4 PBST, the obtained immunosensor was stored at 4 °C prior to use. As control, anti-MC-LR/(Au/MWNTs)/GCE and anti-MC-LR/MWNTs/GCE were prepared with the same procedure.

Analytical Procedure. 10 μL MC-LR solutions with different concentrations or water samples with appropriate dilutions were mixed with 10 μL HRP-MC-LR to obtain the incubation solution. The incubation solution was dropped on the MC-LR immunosensor and incubated for 20 min at 25 °C, and then washed carefully with 0.01 M pH 7.4 PBST to obtain HRP-MC-LR/anti-MC-LR/(Au/CNx-MWNTs)/GCE. During the incubation process the immunosensor was placed in container for avoiding the evaporation of incubation solution. The electrochemical measurement was recorded in 0.2 M PBS solution containing 8.0 mM H_2O_2 and 10 mM *o*-PD. The detection solution was bubbled thoroughly with high purity nitrogen for 10 min and maintained in nitrogen atmosphere. The differential pulse voltammetric (DPV) measurements were from -300 to -850 mV with pulse amplitude of 50 mV and width

of 50 ms. The data for condition optimization and the calibration curve were the average of three measurements.

Characterization of Au/CNx-MWNTs

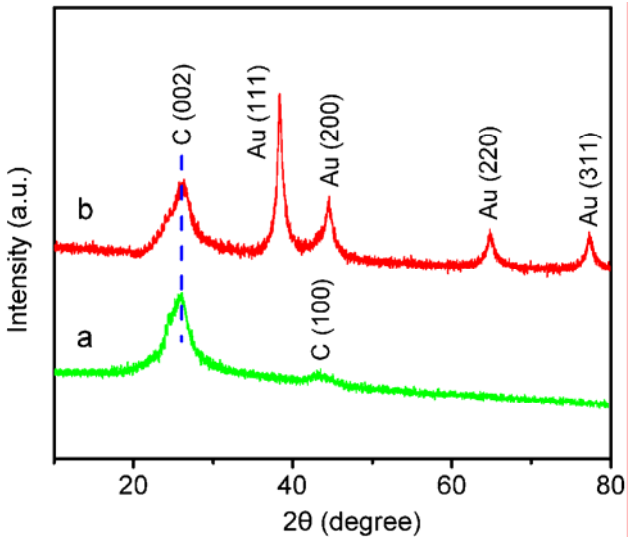

Fig. S1 XRD profiles of (a) CNx-MWNTs and (b) Au/CNx-MWNTs.

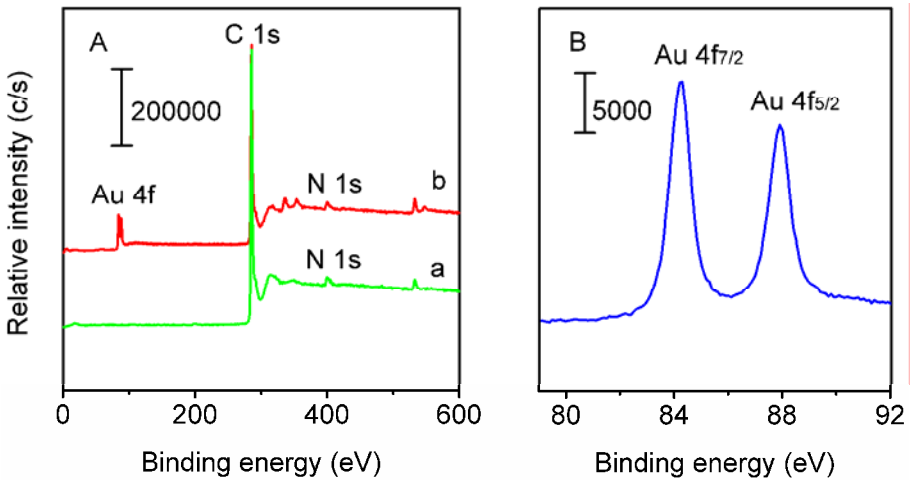

Fig. S2 (A) Survey XPS spectra of CNx-MWNTs (a) and Au/CNx-MWNTs (b), and (B) Au 4f XPS spectrum of Au/CNx-MWNTs.

Optimal Conditions for Immunoreaction

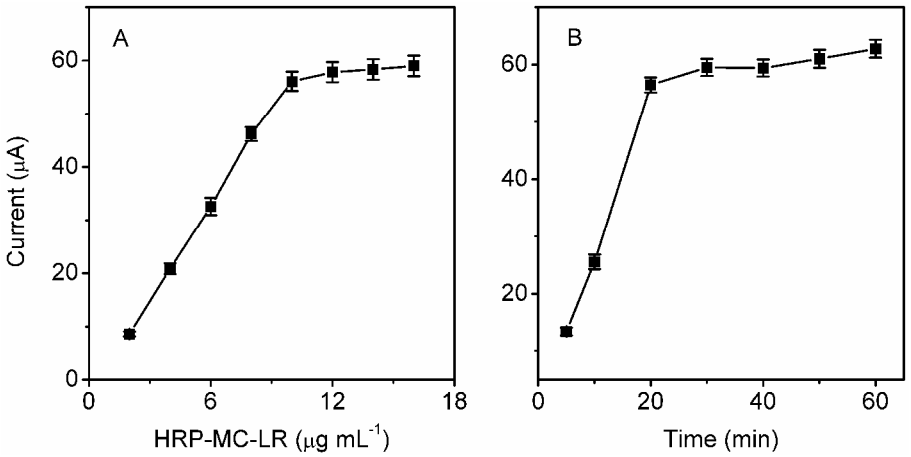

Fig. S3 Effects of (A) HRP-labeled MC-LR concentration and (B) incubation time on amperometric response of HRP-MC-LR/MC-LR/(Au/CNx-MWNTs)/GCE under other optimal conditions.

Optimal Conditions for Detection Solution

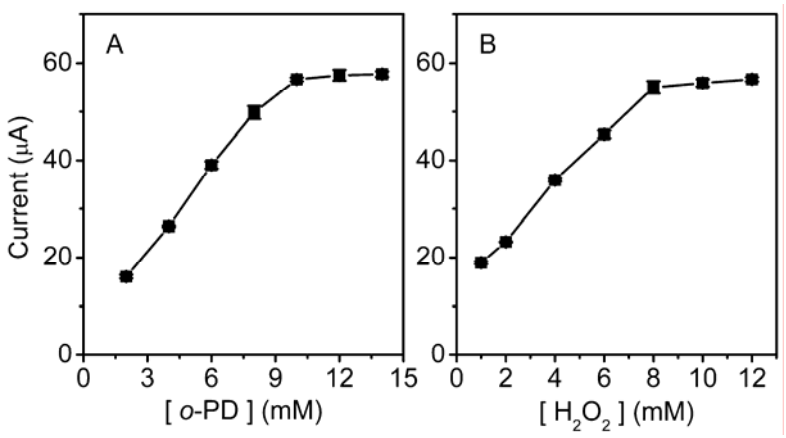

Fig. S4 Effects of (A) *o*-PD and (B) H_2O_2 concentrations on amperometric response of HRP-MC-LR/anti-MC-LR/(Au/CNx-MWNTs)/GCE under other optimal conditions.

References

1 H. Chen, Y. Yang, Z. Hu, K. F. Huo, Y. W. Ma and Y. Chen, *J. Phys. Chem. B*, 2006, **110**,16422–16427.

2 B. Yue, Y. W. Ma, H. S. Tao, L. S. Yu, G. Q. Jian, X. Z. Wang, X. S. Wang, Y. N. Lu and Z. Hu, *J. Mater. Chem.*, 2008, **18**, 1747–1750.